ENVIRONMENTAL ENGINEERING SCIENCE
Volume 19, Number 2, 2002

Effects of Oil and Grease on the Vaporization of Organic Compounds from Contaminated Sediments

R. Ravikrishna, K.T. Valsaraj,* L.J. Thibodeaux, and D.D. Reible

Gordon A. and Mary Cain Department of Chemical Engineering
Louisiana State University
Baton Rouge, LA 70803

ABSTRACT

Contaminated sediments, which contain hazardous compounds such as polynuclear aromatic hydrocarbons (PAHs), are dredged and stored in confined disposal facilities (CDFs). Exposure of the sediment to air results in volatilization of contaminants. Many of the field sediments also contain substantial amounts of oil and grease. An uncontaminated sediment from a local lake (University Lake, Baton Rouge) was spiked with motor oil and PAHs. The air emission flux of three compounds (dibenzofuran, phenanthrene, and pyrene) from the oily sediment was compared to that from the same sediment without oil. The oil content of the sediment was 2.3%, and it had a moisture content of 6.5% to provide 100% pore air relative humidity. Experiments were also conducted with another moisture content of 55% in the sediment. Experiments were performed in dynamic flux chambers in the laboratory. The experimental flux measurements for all three compounds were lowered substantially in the presence of the oil in the sediment. At the end of the experiment, the sediment was cored to obtain the sediment concentration profiles. A mathematical model was constructed based on the hypothesis that the oil served as an additional compartment for the partitioning of the chemicals, and did not contribute an additional layer of resistance to mass transfer resistance from sediments. The comparison of experimental data and the model simulations showed that this hypothesis was true for sediments used in this study, where the oil was immobile.

Key words: oil and grease; sediment; contaminants; vaporization; confined disposal facilities

INTRODUCTION

Contaminated sediments in ports and waterways have to be dredged periodically to make them navigable. The U.S. Army Corps of Engineers dredges several millions of cubic yards of contaminated sediments annually. These are often stored in dike areas called confined disposal facilities (CDFs). A CDF stores contaminated sediments and allows dewatering to occur. The percent moisture content within a CDF may initially be greater than 75% (mass of water per unit mass of wet solids), but drainage and dewatering will occur to field capacity and to near total dryness in the surface layers of dredged material. Because of their exposure to air, the

*Corresponding Author: Ike East Professor of Chemical Engineering, Gordon A. and Mary Cain Department of Chemical Engineering, Louisiana State University, Baton Rouge, LA 70803. *Phone:* 225-578-6522; *Fax:* 225-578-1476; *E-mail:* valsaraj@che.lsu.edu

dredged material within a CDF releases volatile and semivolatile contaminants to the atmosphere at rates that are strong functions of moisture content (Valsaraj *et al.*, 1999). Although few experimental measurements in the field exist, there is a large database on air emissions from exposed sediments in small laboratory microcosms and pilot-scale CDFs (Valsaraj *et al.*, 1997; Chiarenzelli *et al.*, 1998; Valsaraj *et al.*, 1999; Hawthorne and Grabanski, 2000; Ravikrishna *et al.*, 2001).

The air emission from exposed dredged material in a CDF begins with the desorption of contaminants from sediment particles, followed by diffusion of the contaminant as a vapor through the sediment pore air before they emerge into the air boundary layer above the CDF. This process is dependent on the distribution of the contaminant within the various phases in the sediment, a function of the partitioning among the various phases and the volume of those phases. The equilibrium partition constant, K_{sa} (L/kg) between the sediment and pore is given by

$$K_{sa} = \frac{W_S}{C_a} \tag{1}$$

where W_s is the concentration of contaminant on the sediment (mg/kg) and C_a is the pore air concentration of the contaminant (mg/L) at equilibrium. Only few direct experimental measurements of K_{sa} are available in the literature (De Seze *et al.*, 2000a), and in cases where the experimental value of K_{sa} is unavailable it is often obtained from the ratio K_{sw}/H_c, where K_{sw} (L/kg) is the equilibrium sediment/water partition constant, and H_C is the dimensionless Henry's constant (molar concentration ratio). This ratio has been shown to be valid for normal ranges of moisture content (>5%) but may significantly underestimate K_{sa} at very low moisture content (<1%) (De Seze *et al.*, 2000a). In general, a dry (unsaturated) surface has a large capacity for sorption from the vapor phase, whereas a wet (saturated) sediment has a lower capacity of sorption from the vapor phase. A high moisture content sediment, however, also has limited vapor space available. Thus, the maximum vapor flux from sediments would occur at moderate moisture contents where neither the high sorptive capacity of dry sediments nor the limited vapor space in wet sediments would limit vapor movement (Valsaraj *et al.*, 1999).

It was observed in laboratory studies that a clear distinction also existed between contaminated field sediments that contained oil and grease and the laboratory-inoculated sediments that did not (Valsaraj *et al.*, 1999). Oil and grease (OG) is a major component of many field sediments. As shown in Table 1, the OG fraction can approach the total organic carbon fraction in some sediments. The OG is usually measured as total extractable petroleum hydrocarbon, but is poorly characterized for its constituents. The presence of residual petroleum hydrocarbons in sediments and soils has been shown to affect the soil–water and sediment–water partition constants of hydrophobic organic compounds (Boyd and Sun, 1990; Sun and Boyd, 1991; Ortiz *et al.*, 1999). Further, Ortiz *et al.* (1999) showed that the diffusion of polycyclic aromatic hydrocarbons from high viscosity oil to water is controlled by organic phase resistance. It has been suggested that the sediment/water partition constant, K_{sw} (L/kg) for a compound depends on both f_{oc} and f_{oil}, which are, respectively, the fraction organic carbon (OC) on sediment and fraction of OG in the sediment. Partitioning to the OC is characterized by a sediment/water partition constant, K_{oc}, while $K_{oil\text{-}w}$ represents the partition constant between the oil and water. The oily phase has been shown to be as much as 10 times more sorptive than natural organic matter towards polychlorinated biphenyls (PCBs) (Boyd and Sun, 1990). Reduced bioavailability of PCBs due to residual petroleum hydrocarbons in soils and sediments has also been reported (Luthy *et al.*, 1997; Zwiernik *et al.*, 1999).

The above-cited literature indicates that the fate and transport characteristics of HOCs in sediments are likely to be influenced by the presence of oil and grease. The goal of this study was to understand how the volatilization of HOCs from contaminated sediment and dredged materials is affected by the presence of a motor oil. Experiments were conducted using a native, local uncontaminated sediment from the University Lake, Baton Rouge, which was spiked in the laboratory to obtain dif-

Table 1. Fractional oil and grease found in some contaminated sediments and dredged materials.

Sediment type	*Fraction organic carbon*	*Fraction oil and grease*
Indiana Harbor Canal[a]	0.026	0.01
New York Harbor[b]	0.027	0.0003
Grand Calumet River[b]	0.054	0.014
Rouge River, MI[c]	0.04	0.03

[a]From Valsaraj *et al.,* (1999); [b]from Ravikrishna *et al.,* (2001); [c]from Valsaraj *et al.,* (1997).

ferent oil contents and HOC concentrations in the sediment. In separate experiments, sediment with two different moisture contents (6.5 and 55%) were used to compare their behavior with respect to HOC emission fluxes in the presence of oil and grease. Mathematical models were tested with the data obtained from the experiments.

EXPERIMENTAL

Description of apparatus

A flux chamber made of anodized aluminum was used to measure the volatile contaminant emissions. Briefly, the chamber consisted of two parts that were bolted together in an air-tight seal. The top section comprised of an air inlet, an air distribution groove network, a rectangular view glass, another air distribution groove network, and the air outlet, in that order. The air distribution grooves, 3 mm wide and 2 mm deep, were carved into the bottom face of the top section. The bottom section contained a rectangular cavity to hold the sediment that was 4.5 cm long in the direction of flow, 25 cm wide, and 10 cm deep. The mouth of this cavity corresponded to the area of the rectangular view glass in the top section. The detailed design, dimensions of the apparatus, and the experimental setup are described elsewhere (Valsaraj *et al.*, 1999). Compressed air at the desired flow rate (typically 1.7 L/min) is supplied to the inlet of the flux chamber and passed over the sediment surface. Polyaromatic hydrocarbons (PAHs) in the outlet stream were adsorbed on a bed of XAD-2 Resin (Orbo 43, Supelco Inc., PA) connected at the outlet of the flux chamber. A thermohydrometer at the inlet and the outlet were used to measure air relative humidity.

Contaminants and sediments

The flux experiments were conducted using sediment from a local source (University Lake, Baton Rouge, LA). At the time of collection, this sediment was uncontaminated and contained no residual oil or grease. The sediment was inoculated with the contaminants of interest and motor oil as the representative oil phase. The contaminants of concern were polycyclic aromatic hydrocarbons (PAHs) and a heterocyclic aromatic compound (HAC), which are two prevalent classes of contaminants at many contaminated sites. The two PAHs were phenanthrene (PHE) and pyrene (PYR), and the HAC was dibenzofuran (DBF).

Motor oil (Superflo-30, Exxon) was chosen as the representative oil and grease additive in the sediment. It was a substance that was easily available and well characterized. In a study of PAH partitioning to motor oil, Chen *et al.* (1994) noted that approximately 7 million gallons of motor oil make their way into Florida's waterways every year. Therefore, it is likely that lubricating oils represent a significant fraction of the oil and grease ultimately deposited in sediments. Because it is composed mainly of paraffins and naphthenes, we believe that it may be a good surrogate to the poorly characterized oil and grease found in most contaminated sediments. The properties of the contaminants and the oil relevant to this study are given in Table 3.

Preparation of laboratory-spiked sediment

The University lake sediment was obtained using a box-corer and passed through a coarse sieve (2 mm) to remove large-sized stones. Laboratory inoculation of the sediments was performed by introducing about 4 kg of 50% wet (mass by mass) clean sediment solids into 1-gallon glass jars coated with phenanthrene, pyrene, and dibenzofuran on their walls. There was sufficient head space to facilitate mixing of the sediment during the equilibration process. Subsequently, these jars were sealed air tight and tumbled to equilibrate for a period of at least 3 weeks. There was an addition of motor oil to the sediment that was performed either during the inoculation of the contaminants as described above or after the contaminants were equilibrated with the sediment for 3 weeks. Motor oil was introduced directly into the jars containing the sediment in multiple batches of small quantities in all the experiments, except for one, where the oil was introduced in a small amount of hexane solution (<10 mL in 4 kg of wet sediment).

Experiments were conducted with a sediment moisture contents of 6.5 and 55%. De Seze *et al.* (2000b) have previously shown that at 6.5% moisture in the University Lake sediment the pore air relative humidity is $>95\%$. At this moisture content, the contaminant partitioning is predicted well by air–water partitioning, and there is no evidence of strong sorption onto dry mineral surfaces of the solid. The vast majority of the pore space is air filled at this moisture content, encouraging vapor transport. The sediment was initially saturated (55% moisture content) with water during the inoculation process. For the 55% moisture experiments, the inoculated sediment was used as it was. To prepare the 6.5% moisture content sediment, the inoculated wet sediment was subjected to air drying, crushing, and sieving to prepare an unsaturated sediment. The moisture content of the resultant sediment was measured and readjusted to the required level by adding the required amount of water and tumbling for at least 48 h to ensure uniform moisture content. The contaminant concentrations and other relevant properties of the sediment used in the experiment are listed in Table 2.

Table 2. Properties of the sediment.

Sediment property	*Low-moisture sediment*	*High-moisture sediment*
Moisture content, 2w (% g/g)	6.5	55
Fraction organic carbon, f_{oc}	0.026	0.04
Fraction oil, f_{og}	0–0.023	0–0.05
Bulk density, Δ_b (g/cm^3)	0.77	0.72
Total porosity, ϵ_T (cm^3/cm^3)	0.72	0.71
Air-filled porosity, ϵ_a (cm^3/cm^3)	0.67	0.04
Water-filled porosity, ϵ_w (cm^3/cm^3)	0.05	0.67
Dibenzofuran (mg/kg)	38 ± 3	63 ± 4
Phenanthrene (mg/kg)	58 ± 2	96 ± 8
Pyrene (mg/kg)	129 ± 3	136 ± 12

Experimental run

The experimental setup was briefly described in the earlier section and also described in detail elsewhere (Valsaraj *et al.*, 1999). The exposed surface area of sediment was 115 cm^2. In all the experiments, the relative humidity of the inlet air was maintained at 99.9%, except for a brief period when air dried by Drierite® (anhydrous $CaSO_4$) was passed over the sediment. The PAH traps (Orbo 43) at the flux chamber outlet were replaced at the end of every sampling interval, that ranged from 6 to 96 h. At the end of each experiment, the sediment was sectioned into thin layers and analyzed for the contaminant and oil concentration.

Measurement of oil–water partitioning

Batch experiments were performed to measure the equilibrium partitioning of the contaminants of interest between motor oil and water ($K_{\text{oil-w}}$). A stock solution of dibenzofuran, phenanthrene, and pyrene was made in hexane. The solution was filtered and analyzed for its concentration. Stock solution (0.5 mL) was added to 4 g of motor oil and allowed to mix by slow agitation. To this oil layer, about 100 g of deionized water was added. Triplicate samples were placed in a shaker for 96 h to equilibrate. NaCl (0.5 g) was added to each jar, and was set aside for phase separation. About 10 mL of the water layer was drawn out using a syringe and filtered through a 0.7 μm glass fiber filter (GF/F, Whatman). The filtrate was analyzed for the contaminant concentration directly using HPLC with a fluorescence detector.

Analytical methods

The Orbo 43 traps were desorbed using acetonitrile and analyzed by high-performance liquid chromatography (HPLC) according to the NIOSH method 5506 for PAHs (www.cdc.gov/niosh/nmam/pdfs/5506.pdf). The oil in the sediment was measured gravimetrically after Soxhlet extraction using the EPA-SW 846 method 9071. Analysis of contaminant concentration in sediments was performed after sonication extraction according to the EPA-SW 846 method 8310 and subsequent analysis by HPLC. Contaminants in oily sediments were measured after cleanup through a silica gel column according to EPA-SW 846 method 3630 (www.epa.gov/epaoswer/hazwaste/test/main.htm). Moisture content was obtained by measuring the moisture loss from a sample of wet sediment after placing it in an oven at 105°C overnight. Fractional organic carbon was measured both by placing samples in a furnace at 430°C overnight and dividing the mass loss by the van Bemmelen factor (1.7) and also using a CHN analyzer (Perkin-Elmer 2400 Series II). The oil and grease and the fractional content were reported on a dry sediment weight basis.

Experimental flux calculation

The vapor phase contaminant flux (ng · cm^{-2} · h^{-1}) at the sediment surface was calculated using $N_A = (\Delta m_A)/A_c(\Delta t)$ where m_A is the mass of contaminant (ng) collected on the adsorbent during the time interval, Δt (hours) and A_c is the area (cm^2) of the sediment exposed to the overflowing air. For the purposes of comparison and analysis, the flux and sectioning data obtained from all the experiments were normalized to a common loading of 80, 96, and 156 mg/kg for dibenzofuran, phenanthrene, and pyrene, respectively.

MATHEMATICAL MODEL AND HYPOTHESIS

Mechanism of transport in saturated vs. unsaturated sediment

The mechanism of transport of the contaminant from sediment to air depends to a large extent on the amount of water in the sediment (Fig. 1). The water content determines the available pore air space, which in turn, determines the effective diffusivity of the contaminant in the air-filled pore space. At a moisture content of 6.5%, as used in these experiments, the water is largely immobile by capillary forces but the pore air relative humidity is still essentially 100% (De Seze *et al.*, 2000b). At low oil contents, the oil phase is also expected to be immobilized by capillary forces. The bulk of a hydrophobic contaminant would be expected to accumulate in the organic carbon fraction of the sediment and in the oil phase. Direct transfer of a contaminant from both the organic carbon fraction and oil-to-pore air is followed by diffusive mass transport in the pore air to reach the surface (Fig. 1a).

When the sediment is high in water content such that the pore space is water filled, the contaminant will have to diffuse through the pore water before it emerges into the pore air (Fig. 1b). The lighter and less "wetting" oil may also be mobilized at high moisture contents. The oil, being nonvolatile, subsequently may occupy the pore space in the upper sediment layers and provide additional resistance to contaminant diffusion. The associated contaminant movement may thus be influenced by the oil movement and rearrangement within the sediment pores at high moisture contents (water saturated sediments).

We hypothesize that for a sediment with only a small amount of pore water and a relatively large fraction of pore air, oil mobility will not play a role in the transport

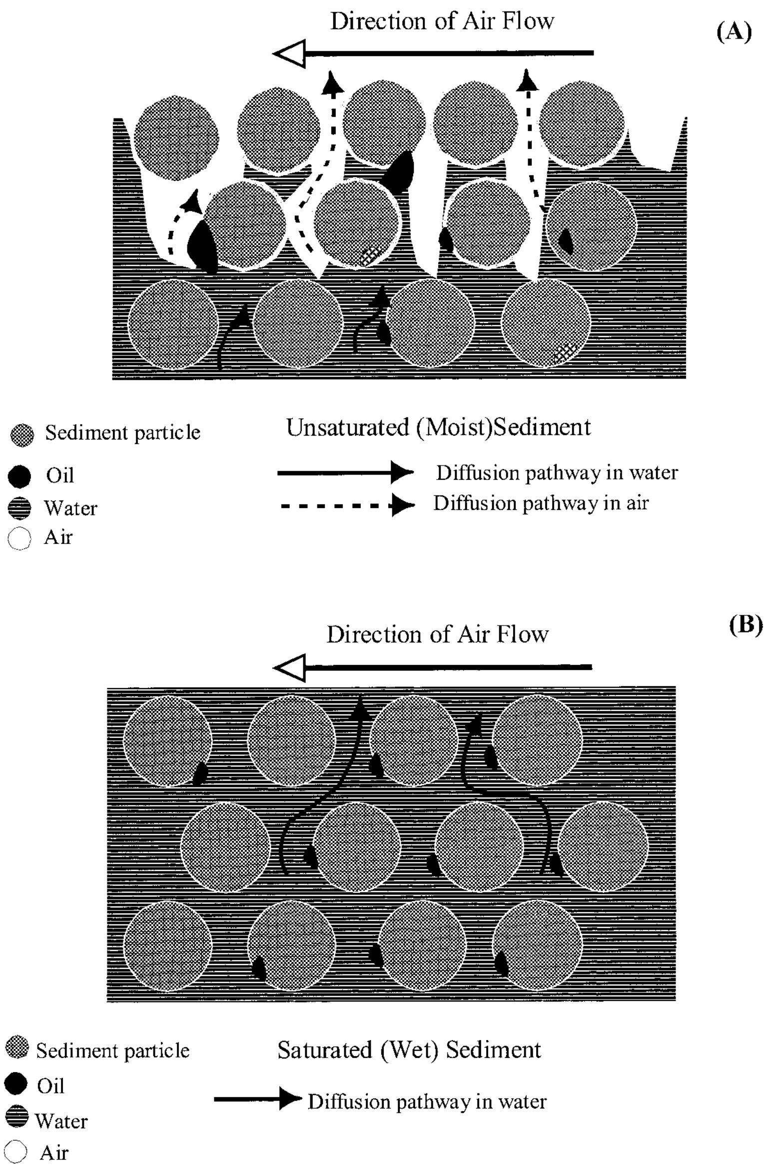

Figure 1. Diffusion pathways for a contaminant in (A) an unsaturated and (B) a saturated sediment containing oil and grease.

of the contaminant; the only contribution in this case will be an additional compartment to which the contaminant will partition. To model the diffusive flux from sediment to air in the presence of oil, we assume local equilibrium to exist for the contaminant between the four phases, viz., pore–air, pore–water, sedimentary organic carbon, and sedimentary oil and grease. A mass balance would give the following for the total mass per unit volume of the sediment:

$$W_S^T = \left(\epsilon_a + \frac{\epsilon_w}{H_C} + \frac{\rho_b f_{\text{oil}} K_{\text{oil-w}}}{\rho_{\text{oil}} H_C} + \rho_b K_{\text{SA}}\right) \cdot C_a = R_F C_a \quad (2)$$

where ϵ_a and ϵ_w are air and water-filled porosities, respectively, ρ_b is the sediment bulk density, ρ_{oil} is the density of the oil and f_{oil} is the fractional oil–grease content. R_F is called the "retardation factor," and represents the ratio of the total mass of contaminant per unit volume of the unsaturated sediment (all phases) to the mass per unit volume of air, which is the only phase in which the contaminant is mobile; that is where significant diffusion or advection may occur. As in groundwater modeling, the capacity of the immobile phases for the con-taminant will slow migration of the mass through the pore space. The air-filled porosity ϵ_a is the ratio of the mass of vapor per unit volume of sediment to the mass of vapor per unit volume of air. The term $(\epsilon_a)/(H_C)$ is the ratio of the mass dissolved in the pore water per unit volume of sediment to the mass of vapor per unit volume of air. Similarly, the terms

$$\frac{\rho_b f_{\text{oil}} K_{\text{oil-}w}}{\rho_{\text{oil}} H_C}$$

and $\rho_b K_{\text{SA}}$ are the ratios of mass sorbed onto the oily phase and the sediment organic carbon, respectively, per unit volume of sediment to the mass of vapor per unit volume of air. The diffusion equation that represents the transport from the sediment is given by

$$R_F \frac{\partial C_a}{\partial_t} = D_{\text{eff}} \frac{\partial^2 C_a}{\partial z^2} \quad (3)$$

The left-hand side of Equation (3) represents the accumulation of contaminant mass in all phases of the sediment–water–oil system, while the right-hand side represents the diffusive transport that occurs through the air phase only. The effective diffusivity, D_{eff}, is given by the Millington-Quirk expression (Millington and Quirk, 1961)

$$D_{\text{eff}} = D_a \frac{\varepsilon_a^{10/3}}{\varepsilon_T^2} \quad (4)$$

with D_a being the molecular diffusivity of the contaminant in air, ε_{T} is the total porosity of the sediment and $\varepsilon_a = (1 - \theta_w)\,\varepsilon_T$ is the air-filled porosity. θ_w is the water content in the sediment. The estimated total porosity in the study was 0.7 and the air-filled porosity was 0.6 for the sediment moisture content of 6.5%. Thus, the moisture and oil in the sediment contribute to the remaining void fraction. The continuum for contaminant transport was clearly the vapor phase, and lends credence to the vapor phase diffusion model presented above.

The solution to the above equation under different boundary conditions has been derived in our previous work (Valsaraj *et al.*, 1999). If a surface (air-side) mass transfer resistance is considered, the flux to air is given by

$$N(t) = C_a^0 k_a \exp\left(\frac{k_a^2 t}{D_{\text{eff}} R_F}\right) \cdot \text{erfc}\left(\frac{k_a^2 t}{D_{\text{eff}} R_F}\right) \quad (5)$$

and the concentration profile within the sediment at any time is given by

$$W_S(z,t) = C_a^0 \frac{R_F}{\rho_b}\left[\text{erf}\left(\frac{R_F z}{\sqrt{4 D_{\text{eff}} R_F t}}\right) + \exp\left(\frac{k_a z}{D_{\text{eff}}} + \frac{k_a^2 t}{D_{\text{eff}} R_F}\right) \cdot \text{erfc}\left(\frac{R_F z}{\sqrt{4 D_{\text{eff}} R_F t}} + k_a \sqrt{\frac{t}{D_{\text{eff}} R_F}}\right)\right] \quad (6)$$

where erfc represents the complementary error function, and k_a is the air boundary layer mass transfer coefficient for the contaminant. If surface (air-side) mass transfer resistance is negligible (i.e., $k_a \to \infty$), the following simple equation for flux results upon differentiation of the simplified Equation (6).

$$N(t) = C_a^0 \sqrt{\frac{D_{\text{eff}} R_F}{\pi \cdot t}} \quad (7)$$

The sediment concentration profile in this case is given by

$$W_S(z,t) = C_a^0 \frac{R_F}{\rho_b}\left[\text{erf}\left(\frac{R_F z}{\sqrt{4 D_{\text{eff}} R_F t}}\right)\right] \quad (8)$$

Verification of the hypothesis

If oil mobility is not expected in sediments, then the oil and grease fraction can be treated as an additional compartment that influences the equilibrium concentration of the contaminant in the pore air or pore water. In the model, this was simply represented by a higher retardation factor (R_f) and a correspondingly lower $C_A{}^0$ (the initial equilibrium concentration of the contaminant in the pore air or pore water). The stated hypothesis can qualitatively be confirmed by the combination of two observations: (a) the reduction in flux in the oily sediments can be explained by the oil and grease fraction incorporated in the model described above, and (b) the oil and grease profile showing no significant relocation of the oil and grease. This same procedure of hypothesis verification can also be extended to the observations with the high moisture sediments.

RESULTS AND DISCUSSION

Experimental flux measurements from 6.5% moisture sediment

Fig. 2(a)–(c) is a plot of the experimental values of flux as a function of time from the start of the experiment for the three compounds, DBF, PHE, and PYR, respectively. In each case two sets of data are presented: one for the control (no oil), and the other where the oil content was 2.3%. The oily and nonoily sediment experiments were conducted with two different batches of contaminated sediment, and hence, their initial concentrations were slightly different. Therefore, for purposes of comparison, the flux was normalized to a common sediment contaminant concentration of 80, 96, and 156 mg/kg, respectively, for DBF, PHE, and PYR. For the case of DBF, the first measured flux without the oil was 373 ng $\cdot$ cm^{-2} $\cdot$ h^{-1} after 12 h, while the corresponding flux in the presence of 2.3% oil was only 125 ng $\cdot$ cm^{-2} $\cdot$ h^{-1} after 22 h. The difference in the first measured fluxes was even more apparent for PHE and PYR. For PHE the first measured flux after 12 h was 72 ng $\cdot$ cm^{-2} $\cdot$ h^{-1} from the nonoily sediment and 9.7 ng $\cdot$ cm^{-2} $\cdot$ h^{-1} after 22 h for the case of the oily sediment. The 12 h flux for PYR was 8.4 ng $\cdot$ cm^{-2} $\cdot$ h^{-1} without the oil, whereas the first measured flux for the case with 2.3% oil was only 0.5 ng $\cdot$ cm^{-2} $\cdot$ h^{-1} after 22 h.

It is clear that the initial fluxes in all the three cases were significantly lower in the presence of oil than the controls. The ratio of the initial flux without oil to that with oil varies from 3 for DBF to 17 for PYR. Note that from Equation (5), the initial flux for a compound is proportional to $k_a C_A{}^0$. Because the initial pore air concen-

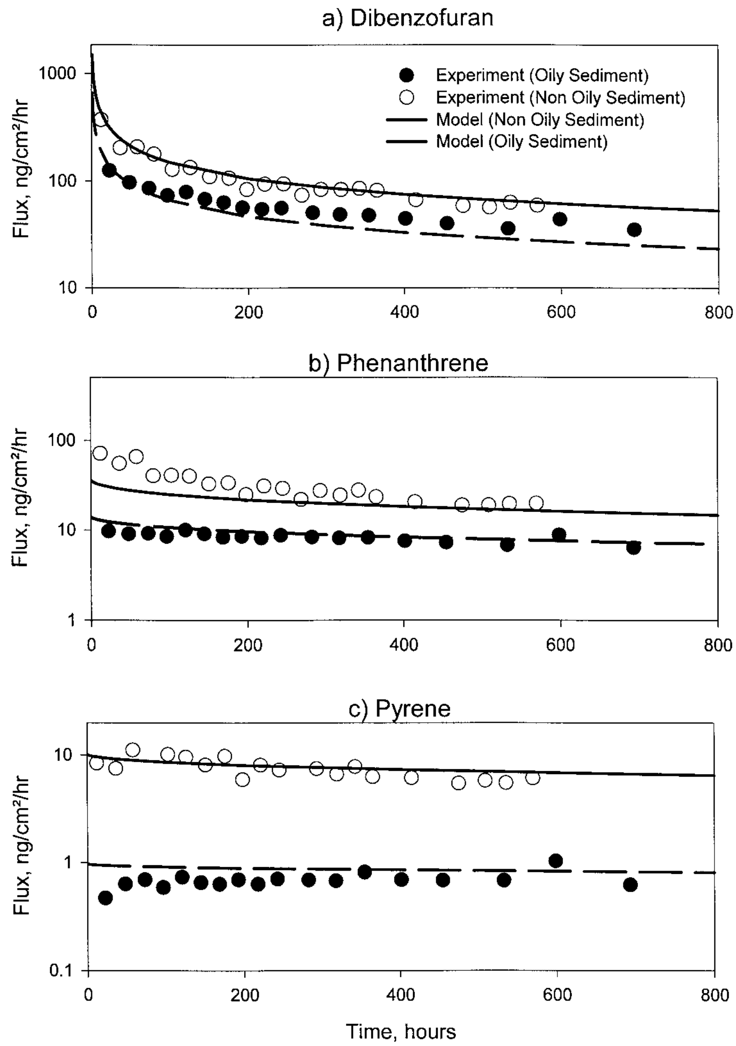

Figure 2. Sediment-to-air flux of dibenzofuran (a), phenanthrene (b), and pyrene (c) from the University Lake sediment containing 2.3% oil and 6.5% moisture content.

tration, $C_A{}^0 = W_S{}^0 \rho_b / R_F$, it is clear that for the same $W_S{}^0$, with increasing R_F as a result of the oil phase, the initial pore air concentration as well as the initial flux for a given compound should decrease. The long-term steady-state fluxes were also similarly affected. For DBF the long-term steady-state flux was 59 ng $\cdot$ cm^{-2} $\cdot$ h^{-1} for the nonoily sediment, while that for the oily sediment was only 35 ng $\cdot$ cm^{-2} $\cdot$ h^{-1}. The long-term fluxes for PHE were 20 and 6.4 ng $\cdot$ cm^{-2} $\cdot$ h^{-1}, respectively for the nonoily and oily sediments. For PYR the long-term steady-state flux was 6.1 ng $\cdot$ cm^{-2} $\cdot$ h^{-1} for the nonoily sediment, whereas that from the oily sediment was only 0.6 ng $\cdot$ cm^{-2} $\cdot$ h^{-1}.

The model-predicted fluxes are also shown in Fig. 2(a)–(c). The difference between the two model predictions presented is the value of the retardation factor. In the first case (control) without oil, the retardation factor assumed f_{oil} equal to zero, whereas in the second case the value of 0.023 was used. The partition constant, viz., K_{sa} was measured earlier from our laboratory (De Seze *et al.*, 2000a), and is given in Table 3. All other necessary parameters in the model are measured values, and are given in Tables 2 and 3. For DBF, the model used was the no-resistance model [Equation (6)], while for both PHE and PYR the surface-resistance model [Equation (4)] was used with a mass transfer coefficient k_a of 0.0008 m/s. This in accordance with the observations from our earlier work (Valsaraj *et al.*, 1999), where we showed that both PYR and PHE have significant air-side resistances, whereas DBF was entirely sediment-side controlled in mass transfer. The model predicted a flux of 473 ng $\cdot$ cm^{-2} $\cdot$ h^{-1} after 10 h, and 61 ng $\cdot$ cm^{-2} $\cdot$ h^{-1} after 600 h for DBF for the nonoily case. The model prediction of DBF flux from the oily sediment was 207 ng $\cdot$ cm^{-2} $\cdot$ h^{-1} after 10 h, and 24 ng $\cdot$ cm^{-2} $\cdot$ h^{-1} after 600 h.

Flux value for PHE generated by the model for the nonoily sediment was 168 ng $\cdot$ cm^{-2} $\cdot$ h^{-1} after 10 h, and 22 ng $\cdot$ cm^{-2} $\cdot$ h^{-1} after 600 h. The predicted flux values for PHE were 13 ng $\cdot$ cm^{-2} $\cdot$ h^{-1} after 10 h, and 8 ng $\cdot$ cm^{-2} $\cdot$ h^{-1} after 600 h for the oily sediment. Flux value for PYR predicted by the model for the nonoily sediment was 9.6 ng $\cdot$ cm^{-2} $\cdot$ h^{-1} after 10 h, and 6.8 ng $\cdot$ cm^{-2} $\cdot$ h^{-1} after 600 h. The predicted flux of PYR for the oily sediment was 0.95 ng $\cdot$ cm^{-2} $\cdot$ h^{-1} after 10 h, and 0.83 ng $\cdot$ cm^{-2} $\cdot$ h^{-1} after 600 h. In each case the value of $K_{\text{oil-w}}$ was adjusted to obtain a better fit between experiment and model. The experimental and fit values of log $K_{\text{oil-w}}$ for each compound are given in Table 4. Best-fit $K_{\text{oil-w}}$ values were about the confidence limits of the measured values shown in Table 4. More importantly, the model predictions indicated that the flux from the oily sediment was three times lower than from the nonoily sediment for DBF. This difference was similar to that observed in the experimental values. Similar observations were true of both PYR and PHE predicted fluxes as well. The retardation factor for the oily sediment was larger than that for the nonoily sediment.

Postexperiment sectioning data of the 6.5% moisture sediment

The sediment was cored into thin sections at the end of the experiment in both cases (oily and nonoily sedi-

Table 3. Dibenzofuran (DBF), phenanthrene (PHE), pyrene (PYR), and motor oil physico-chemical properties.

Contaminant	*DBF*	*PHE*	*PYR*
Aqueous solubility (mg/L)[a]	10	1	0.1
Vapor pressure (mm Hg)[a]	0.0036	0.00025	4.5×10^{-6}
Henry's constant, Hc[a]	0.0031	0.0025	0.00045
Diffusivity in air, D_{a}, (cm^2/s)[a]	0.06	0.058	0.054
Diffusivity in water, D_{w}, (cm^2/s)[a]	6.0×10^{-6}	5.8×10^{-6}	5.5×10^{-6}
Organic carbon–water partition constant,[a] log K_{OC} (L/kg)	4.0	4.4	4.8
Sediment–air partition constant,[b] log K_{sa} (L/kg)	4.87	5.91	6.63

[a]From Thoma (1994); [b]from De Seze *et al.,* (2000b).

Motor Oil (Superflo SAE 30 from Exxon)[c]	
Density, g/cm^3 at 289 K	0.90
Viscosity, cSt at 373 K	10.7
Boiling point, K	564
Average molecular weight	−500
Solubility in water, wt.% at 1 atm	<<0.1
% heavy paraffinic components	>90
% proprietary additives	<10

[c]From Material and Safety Data Sheets (MSDS) on Exxon Web site (www.exxon.com/cgi-bin/bld_frameset.cgi?CONTENT=/exxon_productdata/msds).

Table 4. Experimental and fitted values of the motor oil–water partition constant, log $K_{oil\text{-}w}$ for the three compounds ($K_{oil\text{-}w}$ is dimensionless).

Compound	*Experimental log* $K_{oil\text{-}w} \pm \Phi$	*Model fitted log* $K_{oil\text{-}w}$
Dibenzofuran	4.4 ± 0.1	4.3
Phenanthrene	4.9 ± 0.1	5.1
Pyrene	5.8 ± 0.2	5.9

ments) and the concentration of the contaminants and the oil in each core was determined. Five 2-mm sections were made in the top 1 cm of the sediment, followed by two 5-mm sections and the rest 1 cm or larger sections. Fig. 3(a) and 3(b) show the comparison of contaminant concentration profiles of dibenzofuran and phenanthrene in the oily and nonoily sediments used in the experiments. For purposes of comparison, dibenzofuran and phenanthrene loadings obtained in both the cases were normalized to 80 and 96 mg/kg, respectively. Figure 3(a) shows the dibenzofuran loading as a function of depth from the surface. The open vertical bars represent the loading profile of oily sediment, and the shaded bars represent that of the nonoily sediment. In the nonoily sediment, the first two 2 mm was totally depleted. In the oily sediment, there was only a partial depletion of dibenzofuran that was clearly smaller than the nonoily case. The overall mass of dibenzofuran lost from the nonoily sediment was higher than

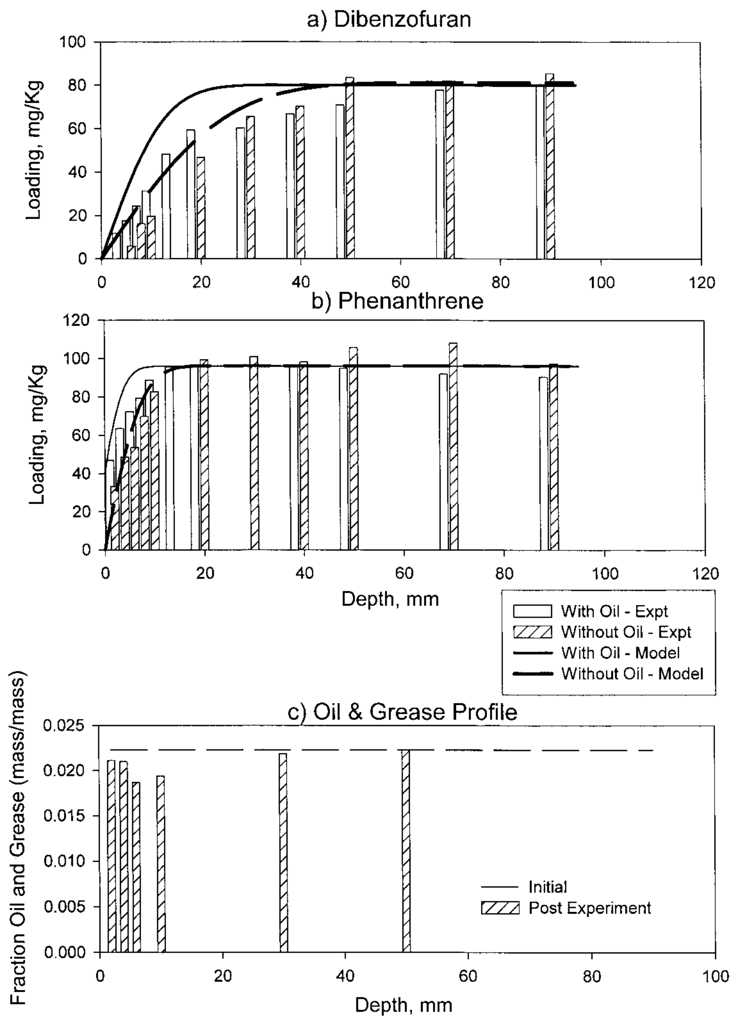

Figure 3. Final concentration profile with depth for dibenzofuran (a), phenanthrene (b), and oil and grease (c) in the University Lake sediment with 6.5% moisture content.

that from the oily sediment. Fig. 3(b) shows a similar comparison for phenanthrene concentration. In both sediments, the loss occurred only from the top 1 cm. The final residual phenanthrene concentration for the nonoily sediment was less than that from the oily sediment, which corroborated the observations from the flux measurements. Table 5 gives the mass balance for DBF and PHE in each case. The percent mass balance ranges from 86 to 96%, affirming the validity of both the flux and core data.

Fig. 3(a) and 3(b) also show the model predictions (solid and broken lines) for the contaminant loading profiles. Equation (8) was used to obtain the profile for dibenzofuran and Equation (6) was used for the phenanthrene profile. These simulations were performed using the same parameters used for the flux prediction in Fig. 2(a)–(c). The simulations showed good agreement with the model. A postexperiment analysis of the oil content of the top few centimeters in the oily sediment revealed no significant loss or relocation of the oil content [Fig. 3(c)].

The reduced experimental fluxes could be modeled by the increased uptake (increased R_F) in the oily phase, and additionally, the sediment sectioning results showed no relocation of the oil phase. These observations together qualitatively confirm the hypothesis stated earlier that oil and grease serve only as a compartment to which contaminant sorption occurs.

Experimental flux measurements for 55% moisture sediment

Fig. 4(a) and 4(b) shows, respectively, the flux of DBF and PHE from the 55% moisture sediment. Pyrene was also present in the sediment during the experiments, but the PYR data were discarded, owing to some unexplainable problems in them. As in the low moisture content experiment, the flux and the sectioning comparison were performed with normalized loading for DBF and PHE. Fig. 4(a) shows the comparison of DBF flux from oily and nonoily sediments. DBF flux from the oily sediment was 39 $ng \cdot cm^{-2} \cdot h^{-1}$ after 7 h, 7 $ng \cdot cm^{-2} \cdot h^{-1}$ after 60 h and was constant for the next 80 h. In the period up to 140 h, the sediment consolidated, and because there was no evaporation of water, the ejected porewater collected on top of the sediment in a water film 6–7-mm thick. The constant flux during this time was a measure of evaporation of DBF from this overlying water surface. This accumulation of water at the surface was also observed in the concurrent experiment with the nonoily sediment. At this point (after 140 h), the experiment was interrupted and the overlying water layer was removed by a pipette carefully from both the chambers. The experiment was restarted after this and the DBF flux increased to 15 $ng \cdot cm^{-2} \cdot h^{-1}$ from the oily sediment, gradually reducing to 8.6 $ng \cdot cm^{-2} \cdot h^{-1}$ after 530 h and 5.6 $ng \cdot cm^{-2} \cdot h^{-1}$ after 1400 h.

The PHE flux before water removal was 5.31 $ng \cdot cm^{-2} \cdot h^{-1}$ after 7 h, and 1.8 $ng \cdot cm^{-2} \cdot h^{-1}$ after 140 h. After the water removal, the flux increased to 4.3 $ng \cdot cm^{-2} \cdot h^{-1}$ after 241 h and then gradually decreased to 3.2 $ng \cdot cm^{-2} \cdot h^{-1}$ after 530 h and 1.9 after 1400 h. For the nonoily sediment, the DBF flux was 47 $ng \cdot cm^{-2} \cdot h^{-1}$ after 7 h from the start, and 17 $ng \cdot cm^{-2} \cdot h^{-1}$ after 140 h. After water removal, the flux increased to 24 $ng \cdot cm^{-2} \cdot h^{-1}$ and

Table 5. Mass balance from the flux and core data.

	DBF		*PHE*	
	Without oil	*With oil*	*Without oil*	*With oil*
6.5% moisture sediment				
Initial mass from loading data, mg	35.4	34.7	53.3	36.6
Final mass from the coring data, mg	28.5	27.6	49.4	31.7
Mass volatilized from flux data, mg	4.3	2.3	1.6	0.5
Percent mass balance	93%	86%	96%	88%
55% moisture sediment				
Initial mass from loading data, mg	36.2	25.2	51.3	48.8
Final mass from the coring data, mg	33.8	24.2	49.5	45.6
Mass volatilized from flux data, mg	2.2	1.0	1.0	0.4
Percent mass balance	99%	100%	98%	94%

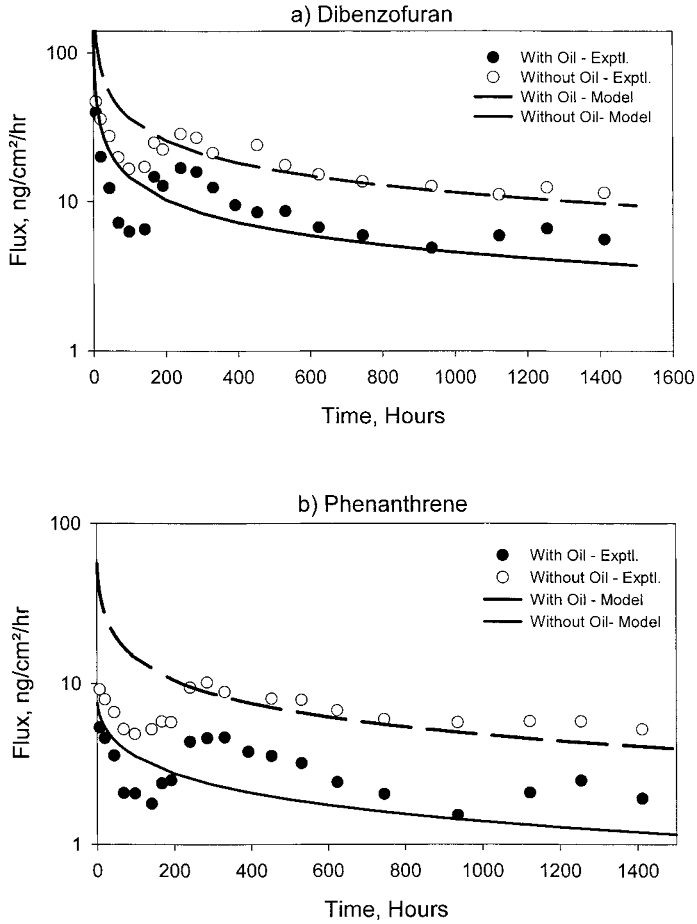

Figure 4. Sediment-to-air flux of dibenzofuran (a), and phenanthrene (b), from the University Lake sediment containing 2.3% oil and 55% moisture content.

then gradually decreased to 18 ng $\cdot$ cm^{-2} $\cdot$ h^{-1} in 530 h and 11 ng $\cdot$ cm^{-2} $\cdot$ h^{-1} after 1400 h. The PHE flux before water removal was 9.1 ng $\cdot$ cm^{-2} $\cdot$ h^{-1} after 7 h from the start, and 5.2 ng $\cdot$ cm^{-2} $\cdot$ h^{-1} after 140 h. After the removal of the water film, the flux increased to 9.4 ng $\cdot$ cm^{-2} $\cdot$ h^{-1} in the next 100 h and then gradually decreased to 7.9 ng $\cdot$ cm^{-2} $\cdot$ h^{-1} after 530 h and 5.2 ng $\cdot$ cm^{-2} $\cdot$ h^{-1} after 1400 h. There was a consistent difference between the flux from the oily and nonoily sediments.

Fig. 4(a) and 4(b) also shows the model prediction of the flux. The model assumed diffusion in the water phase and retardation from the water phase, because water was the dominant medium in the pores. The models shown in Equations (4)–(8) were used. The retardation factor was recomputed assuming no air phase (i.e. $\epsilon_a = 0$) in the mass balance indicated by Equation (2). The effective diffusivity were computed using the Millington and Quirk's expression [Equation (4)] using the water-filled porosity and the diffusivity of the contaminants in water. Consequently, the concentration terms (C_a) in Equation (5)–(8) were the pore water concentrations. Also, the air-side mass transfer coefficient, k_a, in Equations (5) and (6) was corrected by multiplying with a factor H_c, the Henry's constant. This assumed rapid equilibrium at the air–water interface. The model predictions were performed with the sediment properties estimated after the water removal, and therefore, the predictions agreed with the experimental flux after the first 200 h, when the experiment was restarted after water removal. The $K_{\text{oil-w}}$ values used were the model fit values shown in Table 4. The models and boundary conditions used to obtain flux for DBF and PHE were the same as used in the 6.5% moisture sediment case discussed in the previous section. The DBF model assumed no air-side resistance, while the PHE model assumed a finite mass transfer resistance. The difference in the experimental data between the oily and nonoily sediments was similar to the differences in

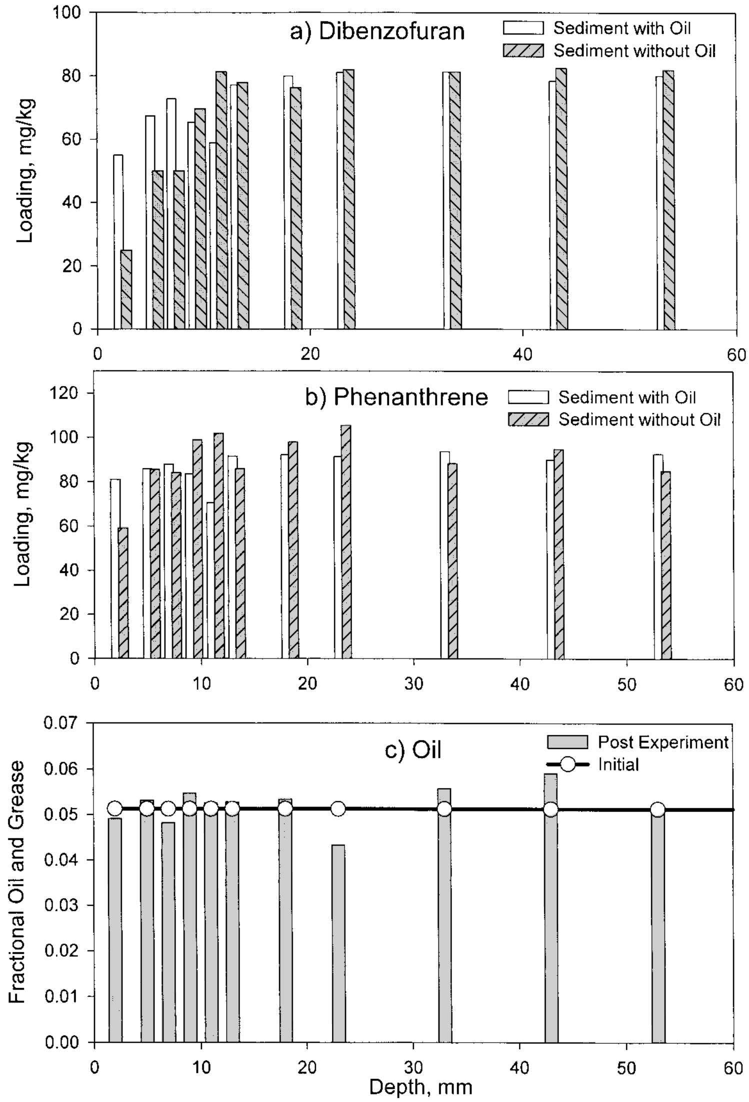

Figure 5. Final concentration profile with depth for dibenzofuran (a), phenanthrene (b), and oil (c) in the University lake sediment with 55% moisture content.

their model prediction. This suggests sorption of the contaminants to oil phase.

Postexperiment sectioning data for 55% moisture sediment

Fig. 5(a)–(c) shows, respectively, the postexperiment sediment sectioning data for DBF, PHE, and the oil. Further evidence for this comes from Fig. 5(a)–(c). Fig. 5(a) and 5(b) show the postexperiment sectioning data for DBF and PHE, respectively. The surface section was about 3 mm thick, followed by five 2-mm sections, two 5-mm sections, and the remainder 10-mm sections. The depletion in the nonoily sediments in the surface layers was greater than the oily sediments, indicating more loss from the former. The overall mass balance shown in Table 5 ranged from 94 to 100%, validating the flux and sectioning data. Fig. 5(c) shows the profile of the measured oil and grease in the postexperiment sections. There was no definitive gradient or trend of oil and grease values obtained and the comparison with the initial values show that there was no movement of the oil in the sediment.

The observations from the flux data and the absence of any oil relocation in the high moisture sediment again qualitatively confirms the hypothesis and the assumption that the decreased flux of the contaminants can be explained only by sorption to the oil and grease phase alone, and negates the possibility of any other resistance to mass transport such as the accumulation of a cap-like oil film near the sediment surface due to oil movement. However, the analysis presented here applies only to situations of constant sediment properties. When water-saturated oily sediments are allowed to dry, it results in the rapid movement of water towards the sediment–air interface. It would be interesting to investigate the response of the oil phase in such a scenario.

CONCLUSIONS

Experimental data for both the 6.5 and 55% moisture content sediments showed reduction of contaminant fluxes at the surface of exposed sediments in the presence of oil and grease. Model predictions that accounted for the sorption to the oil–grease phase, in combination with the lack of oil and grease relocation observed in the postexperiment sediment sectioning data, strongly suggested that the oil phase imply acted as an additional compartment for the contaminant sorption. Other retarding mechanisms such as diffusional barrier caused by a mobilized oil film near the sediment surface were discounted in the conditions under which the experiments were performed. Other environmental conditions in statics sediment systems such as evaporation of water at the surface or movement of water above the surface may induce oil mobility. Further studies are warranted to verify these mechanisms.

ACKNOWLEDGMENTS

This work was supported partly by the U.S. EPA through the Hazardous Substance Research Center (S&SW), and by the U.S. Army Corps of Engineer Waterways Experiment Station through the Long-Term Effects of Dredging (LEDO) program.

REFERENCES

BOYD, S.A., and SUN, S. (1990). Residual petroleum and polychlorinated biphenyl oils as sorptive phases for organic contaminants in soils. *Environ. Sci. Technol.* **24,** 142.

CHEN, C.S.H., DELFINO, J.J., and RAO, P.S.C. (1994). Partitioning of organic and inorganic components from motor oil into water. *Chemosphere* **28,** 1385.

CHIARENZELLI, J., SCRUDATO, R., BUSH, B., CARPENTER, D., and BUSHART, S. (1998). Do large scale remedial and dredging events have the potential to release significant amounts of semivolatile compounds to the atmosphere? *Environ. Health Perspect.* **106,** 47.

DE SEZE, G., VALSARAJ, K.T., REIBLE, D.D., and THIBODEAUX, L.J. (2000a). Sediment–air equilibrium partitioning of hydrophobic organic compounds. 2. Saturated vapor pressures, and the effects of sediment moisture content and temperature on the partitioning of phenanthrene and dibenzofuran. *Sci. Tot. Environ.* **253,** 27.

DE SEZE, G., VALSARAJ, K.T., REIBLE, D.D., and THIBODEAUX, L.J. (2000b). Sediment–air equilibrium partitioning of hydrophobic organic compounds. 1. Method development and water vapor sorption isotherms. *Sci. Tot. Environ.* **253,** 15.

HAWTHORNE, S.B., and GRABANSKI, C.B. (2000). Vaporization of polycyclic aromatic hydrocarbons from sediments at ambient conditions. *Environ. Sci. Technol.* **34,** 4348.

LUTHY, R.G., DZOMBAK, A., SHANNON, M.J.R., UNTERMAN, R., and SMITH, J.R. (1997). Dissolution of PCB congeners from an aroclor and an aroclor/hydraulic oil mixture. *Water Res.* **31,** 561.

MILLINGTON, R.J., and QUIRK, J.P. (1961). Permeability of porous solids. *Trans. Faraday Soc.* **57,** 1200.

ORTIZ, E., KRAATZ, M., and LUTHY, R.G. (1999). Organic phase resistance to dissolution of polycyclic aromatic hydrocarbon compounds. *Environ. Sci. Technol.* **33,** 235.

RAVIKRISHNA, R., VALSARAJ, K.T., REIBLE, D.D., THIBODEAUX, L.J., PRICE, C.B., BRANNON, J.M., MYERS, T.E., and YOST, S. (2001). Air emission flux from contaminated dredged materials stored in a pilot-scale confined disposal facility. *J. Air Waste Managmt. Assoc.* **51,** 174.

SUN, S., and BOYD, S.A. (1991). Sorption of polychlorinated biphenyls congeners by residual PCB–oil phases in soils. *J. Environ. Qual.* **20,** 557.

THOMA, G.J. (1994). Studies on diffusive transport of hydrophobic organic chemicals in bed sediments. Ph.D. Dissertation, Louisiana State University, Baton Rouge, LA.

VALSARAJ, K.T., CHOY, B., RAVIKRISHNA, R., REIBLE, D.D., THIBODEAUX, L.J., PRICE, C.B., BRANNON, J.M., and MYERS, T.E. (1997). Air emissions from exposed, contaminated sediments and dredged materials 1. Experimental data in laboratory microcosms and mathematical modeling. *J. Hazard. Mater.* **54,** 65.

VALSARAJ, K.T., RAVIKRISHNA, R., CHOY, B., THIBODEAUX, L.J., REIBLE, D.D., PRICE, C., YOST, S., BRANNON, J.M., and MYERS, T.E. (1999). Air emissions from exposed contaminated sediments and dredged materials. *Environ. Sci. Technol.* **32,** 142.

ZWIERNIK, M.J., QUENSEN, J.F., and BOYD, S.A. (1999). Residual petroleum in sediments reduce the bioavailability and rate of reductive dechlorination of aroclor 1242. *Environ. Sci. Technol.* **33,** 3574.